Detection and Classification of Crystallographic Defects in Wide Bandgap Semiconductor Materials for Next-Generation Power Switching Devices

Crystallographic defects, especially dislocations in the wide bandgap semiconductors SiC, GaN and AlN, have been revealed and classified using X-ray topography (XRT). By analyzing the geometrical features and the appearances of the dislocation-related contrasts in XRT images, dislocation density, dislocation types in terms of the Burgers vector and their distribution across the entire wafer were obtained.

GaN, SiC and AlN are good candidates for the fabrication of next-generation power switching devices that can operate at high voltage and large current, owing to their remarkable physical properties [1]. However, crystallographic defects, especially dislocations, in these materials are detrimental as they strongly affect the device performance, lifetime and reliability [2, 3]. It is therefore important to reveal and classify dislocations in bulky substrates and epitaxial layers to develop dislocation reduction strategies for crystal growth and for understanding the role that each type of dislocation plays in power devices.

Synchrotron X-ray topography (XRT) is a nondestructive technique to observe dislocations in these materials. It provides a two-dimensional intensity mapping of the X-rays diffracted by a crystal. Because the distortion of crystal planes around a dislocation results in a diffraction direction different to that of the host matrix, dislocations can be visualized by forming contrast different to the background of the defect-free area. A schematic drawing of the experimental setup and principle of XRT observation is shown in Fig. 1. In this report, observation of dislocations in GaN [4] is described as an example; similar observations were carried out for SiC and AlN, which also have a hexagonal crystal structure [5, 6].

A commercial ammono-thermal GaN sample was observed. X-ray diffraction (XRD) measurements showed a radius of curvature of {0001} planes greater than 100 meters. This large radius of curvature is an indispensable characteristic for XRT observation. Synchrotron monochromatic-beam XRT (λ = 1.127 Å) was recorded from the CMP-treated Ga-face. Asymmetric diffractions with six equivalent diffraction vectors ***g*** of 11–26 were applied by rotating the sample every 60° with respect to its surface normal, in addition to a symmetric diffraction with ***g*** = 0008. Diffraction planes (visualized by VESTA [7]) are shown in Fig. 1. Nuclear emulsion plates were used to record XRT images. The topmost 10 μm of the surface of the sample makes a major contribution to the XRT images.

Dislocations in GaN are mainly threading dislocations (TD) propagating nearly along the c-axis. They can be categorized into edge-type (ED, ***b*** = m*a*), screw-type (SD, ***b*** = n*c*), and mixed-type (MD, ***b*** = n*c*+m*a*, n, m = 1, 2, ...), according to their Burgers vectors. Spot-shaped contrasts in all seven XRT images (not shown) taken with six equivalent g-vectors of 11–26, and ***g*** = 0008 have been found to have a one-to-one correlation in position. According to the ***g***·***b*** invisibility criterion (***g*** is the diffraction vector and ***b*** the Burgers vector), images taken with ***g*** = 11–26 should reveal all three types of TDs,

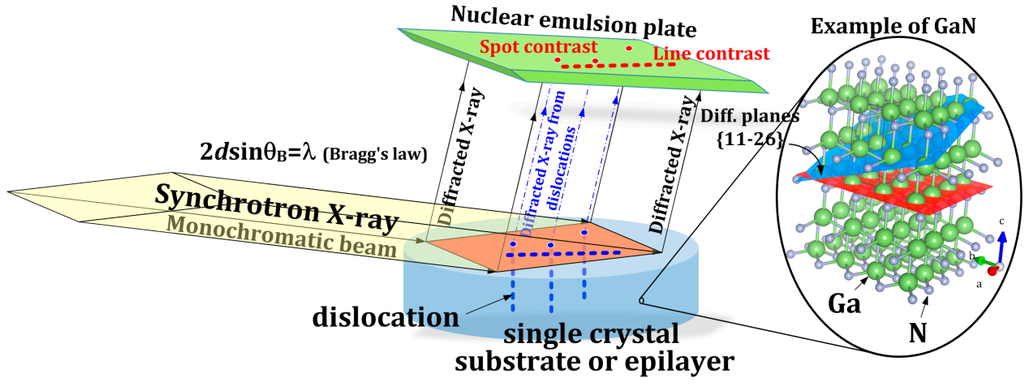

Figure 1: A schematic drawing of the experimental setup and principle of XRT observation. An example of GaN is shown using crystal planes of {11–26} as the diffraction plane.

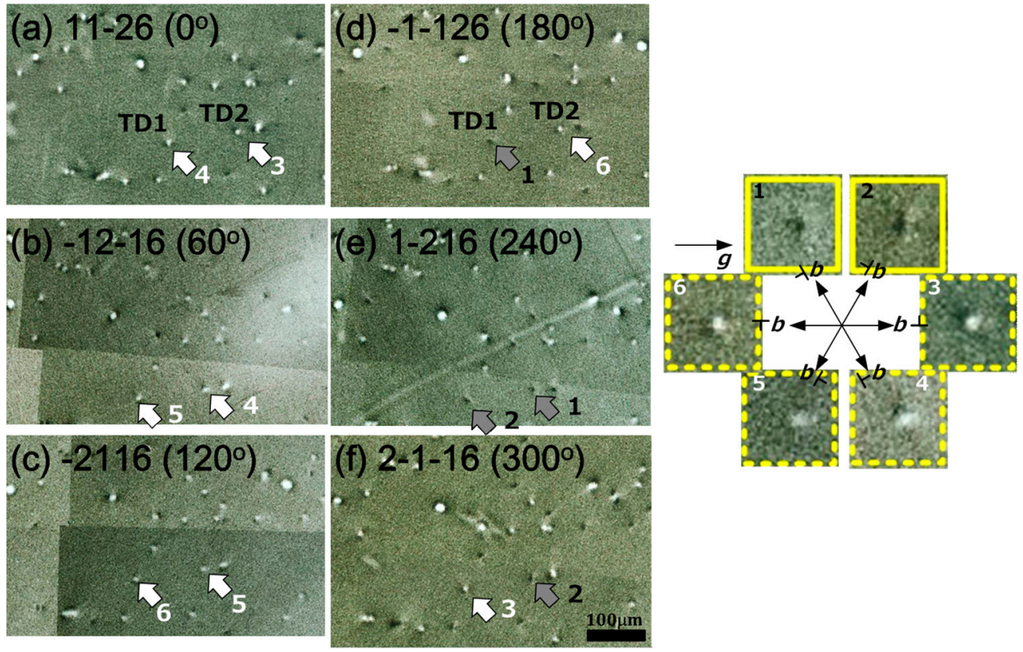

Figure 2: Changes in dark/bright contrast of *c*+*a* TD spots when ***g***-vectors are changed among six equivalent 11–26 from (a) to (f).

while the image with ***g*** = 0008 should reveal TDs whose ***b*** contains a c-component (SD or MD). This result indicates that there are no pure EDs in this sample. Most of the TDs (~96%) are MDs with ***b*** = <11–20>/3+<0001>, the so-called c+a dislocations. Only a very small percentage (~1%) of TDs is pure 1*c* SD with ***b*** = <0001>. The other 3% are TDs containing *c*-component Burgers vector no smaller than 2*c*.

In GaN, not only the magnitude but also the direction of the Burgers vectors provides important feedback to the crystal growth. This information can be acquired from the contrast change in the XRT images. Figure 2 shows the change in dark/bright contrast of *c*+*a* TD spots when ***g***-vectors are changed among six equivalent 11–26 (phi changes from 0° to 300° every 60°). Using TD1 as an example, it first appears as a dark spot in Fig. 2(d) and then Fig. 2(e), and appears as a bright spot in the other four images. TD2 shows similar results with 60° difference in in-plane rotation angle φ. Comparing with the XRT spot contrast for threading edge dislocations in 4H-SiC [8], it is clear that the changes in dark or bright contrast ("2 dark+4 bright") originate from the direction of the *a*-component of ***b*** with respect to the applied ***g***-vector. Thus, the direction of the *a*-component of *c*+*a* TDs in GaN can be unambiguously determined.

In this way, dislocations can be revealed over a wide sample area. Moreover, dislocation types can be determined by analyzing the dislocation-related contrast. Not only edge-, screw- and mixed-type dislocations can be identified, but also the direction of the *a*-component in mixed-type dislocations can be accurately determined. These results provide important information for improving crystal growth as well as for analyzing failures in power devices.

REFERENCES

[1] S. Fujita, *Jpn. J. Appl. Phys.* **54**, 030101 (2015).
[2] H. Matsuhata and T. Sekiguchi, *Philos. Mag.* **98**, 878 (2018).
[3] T. Kachi and T. Uesugi, *Sensor Mater.* **25**, 219 (2013).
[4] Y. Yao, Y. Ishikawa, Y. Sugawara, Y. Takahashi and K. Hirano, *J. Electron. Mater.* **47**, 5007 (2018).
[5] Y. Yao, Y. Ishikawa, Y. Sugawara, K. Sato, K. Danno, H. Suzuki, T. Bessho, S. Yamaguchi and K. Nishikawa, *J. Cryst. Growth* **364**, 7 (2013).
[6] Y. Yao, Y. Sugawara, Y. Ishikawa, N. Okada, K. Tadatomo, Y. Takahashi and K. Hirano, *Jpn. J. Appl. Phys.* **58**, SCCB29 (2019).
[7] K. Momma and F. Izumi, *J. Appl. Crystallogr.* **44**, 1272 (2011).
[8] I. Kamata, M. Nagano, H. Tsuchida, Y. Chen and M. Dudley, *Mater. Sci. Forum* **600-603**, 305 (2009).

BEAMLINES

BL-3C and BL-14B

Y. Yao[1], Y. Sugawara[1], Y. Ishikawa[1], Y. Takahashi[2] and K. Hirano[3] ([1]Japan Fine Ceramics Center, [2]Nihon Univ., [3]KEK-IMSS-PF)